Journal of Molecular Structure 1340 (2025) 142600

Contents lists available at ScienceDirect

Journal of Molecular Structure

journal homepage: www.elsevier.com/locate/molstr

Molecular diversity of bioactive compounds from horned melon peel: Solvent dynamics, antibacterial activity against multidrug-resistant *Pseudomonas aeruginosa* and *in silico* interactions with virulence factors

Mladen Rajaković [a], Uroš Gašić [a], Danka Bukvički [b], Mirjana Pešić [c], Danijel Milinčić [c], Jovana Petrović [a], Ivana Sofrenić [d], Carlos S.H. Shiraishi [e,f], Dejan Stojković [a,*]

[a] Institute for Biological Research "Siniša Stanković", National Institute of the Republic of Serbia, University of Belgrade, Bulevar Despota Stefana 142, Belgrade 11108, Serbia
[b] Faculty of Biology, University of Belgrade, Studentski trg 16, 118, Belgrade 11158, Serbia
[c] Institute of Food Technology and Biochemistry, Faculty of Agriculture, University of Belgrade, Nemanjina 6, Belgrade 11080, Serbia
[d] Faculty of Chemistry, University of Belgrade, Studentski trg 12-16 118, Belgrade 11158, Serbia
[e] CIMO, LA SusTEC, Instituto Politécnico de Bragança, Campus de Santa Apolónia, Bragança 5300-253, Portugal
[f] Nutrition and Bromatology Group, Department of Analytical Chemistry and Food Science, Instituto de Agroecoloxía e Alimentación (IAA), Universidade de Vigo – CITEXVI, Vigo 36310, Spain

ARTICLE INFO

Keywords:
C. metuliferus
Antibacterial
Molecular docking
Ultrasound-assisted extraction
Pseudomonas aeruginosa

ABSTRACT

This study examines chemical composition and the antibacterial properties of various hydro-ethanolic extracts of *Cucumis metuliferus* E. Mey peel against the multidrug-resistant pathogen *Pseudomonas aeruginosa*. Several parameters, including ethanol concentration, extraction time, and ultrasonic power, were used in the ultrasound-assisted extraction of *C. metuliferus* peel. UHPLC-QToF-MS analysis was used to explore the molecular diversity of bioactive compounds in the sample extracts (25 in total), identifying nine hydroxybenzoic acid derivatives and eleven other compounds. Furthermore, antibacterial activity of these extracts was determined. Four of the tested extracts exhibited promising antibacterial properties, with MIC value 0.25 mg/mL and MBC value 0.5 mg/mL. Molecular docking simulations were employed to identify bioactive compounds within the extracts that target some *P. aeruginosa* virulence factors, specifically elastase B and lipase A. The results revealed that several compounds, including decaffeoyl-acteoside, as well as derivatives of vanillic and hydroxybenzoic acids, exhibited strong binding affinities to both enzymes, suggesting their promising potential as inhibitors of *P. aeruginosa* virulence. Furthermore, decaffeoyl-acteoside exhibited high binding affinity for both enzymes, highlighting its potential as a dual-target therapeutic agent. The study effectively leverages solvent dynamics to maximize the extraction and bioactivity of *C. metuliferus* peel compounds. It provides a clear demonstration of how manipulating solvent conditions can influence molecular interactions, extraction yield, and the functional properties of bioactive compounds. The obtained results regarding promising antibacterial and virulence-inhibiting qualities support further research into *C. metuliferus* peel compounds as a natural alternative to traditional antimicrobial treatments.

1. Introduction

Cucumis metuliferus E. Mey, also known as kiwano, jelly melon, thorn melon, bitter wild cucumber, and melanom [1] is a member of the Cucurbitaceae family which includes approximately 120 genera and over 800 species [2], with diverse applications, including medicinal and nutritional. It is also utilized for biodiesel production, as food ingredients, for aqua feed and poultry [2], as well as in the pharmaceutical and cosmetics industries [3]. Given its bitter taste, some authors suggest that *C. metuliferus* may be the most primitive species of *Cucumis*, with other species, such as *Cucumis melo,* deriving from it [4]. Thorn melon is a monoecious annual plant that uses tendrils opposite to leaves to climb. The staminate (male) flowers typically appear before the pistillate (female) flowers. It grows at altitudes ranging from 210 m to

* Corresponding author.
E-mail address: dejanbio@ibiss.bg.ac.rs (D. Stojković).

https://doi.org/10.1016/j.molstruc.2025.142600
Received 20 December 2024; Received in revised form 30 April 2025; Accepted 5 May 2025
Available online 6 May 2025

1800 m above sea level, and flowers from July to September, with fruits ripening between October and December [5]. The green, unripe fruit covered with blunt spines, turns orange upon ripening and measures approximately 12 cm in length and 8 cm in diameter. Mesocarp of the fruit is green and juicy, containing ellipsoid-shaped edible seeds that are approximately 5 to 9 mm long [6].

Despite ongoing efforts to reduce the misuse and overuse of antibiotics, drug-resistant bacterial strains continue to pose a significant global health threat. Combined with the slow pace of developing new, effective antimicrobials, this issue leads to approximately 25,000 deaths caused by multidrug-resistant bacteria annually in Europe and 23,000 in the United States. This high mortality highlights the urgent need for the discovery of novel therapeutics, with naturally sourced substances emerging as an important source of bioactive compounds with potential in drug development [7]. Among resistant strains, *Pseudomonas aeruginosa* can induce chronic infections in patients with ventilator-associated pneumonia, cystic fibrosis, and hospital-acquired infections. This opportunistic pathogen is characterized by a large genome which allows it to adapt rapidly and acquire resistance through various mechanisms [8]. Furthermore, it possesses multiple virulence mechanisms that increase its capacity to cause severe infections, including secreted toxins (ExoS, ExoT, ExoY), extracellular factors like elastase B and lipase A, and biofilm formation [9–13]. Elastase B (LasB), a multifunctional metalloenzyme induces hemorrhage and digests extracellular matrix components [12], while lipase A (LipA) degrades the host cell membrane [14], and supports biofilm formation [15].

Given the aforementioned challenges in eradicating *P. aeruginosa* as well as other multi-drug resistant strains, there is a pressing need for new platforms that incorporate the latest and the most efficient research to accelerate the development of therapeutic treatments for challenging infections caused by these resistant bacteria [16].

Recently, *in silico* methods have emerged as an efficient and cost-effective approach for rapid screening of compounds with potential in novel drug development. This approach is primarily used to evaluate potential drug candidates by simulating their interactions with various biological targets. In case of *P. aeruginosa*, this method identifies compounds that target its virulence factors, offering a potential novel strategy to combat its resistance to currently used antibiotics. By focusing on these virulence factors, the goal is to reduce the pathogenicity of *P. aeruginosa*. This could enable the development of compounds that complement antibiotics — or, more importantly, directly inhibit virulence factors to eradicate the pathogen. Eventually, this may reduce our reliance on traditional antimicrobial treatments and decrease the of resistant strains.

Given the urgent need for novel and cost-effective strategies to treat *P. aeruginosa*, this study investigated the potential of an non-edible plant as a source of bioactive compounds for bacterial eradication. More specifically, antibacterial properties of hydro-ethanolic extracts from horned melon peel were evaluated against the multidrug-resistant pathogen *P. aeruginosa*. In addition, the various parameters of ultrasound-assisted extraction—such as ethanol concentration, extraction time, and ultrasonic power—were optimized to determine the conditions that maximize antimicrobial effects. Furthermore, chemical characterization of the extracts using UHPLC-QToF-MS and molecular docking simulations were conducted to explore the potential of the identified compounds as inhibitors of *P. aeruginosa* virulence factors, such as elastase B and lipase A.

2. Materials, methods, and *in sillico* simulations

2.1. Plant material

Ripe fruits of the *C. metuliferus* E. Mey (Cucurbitaceae) were collected from a local grower in Bogatić, Serbia, during September 2022 and kept refrigerated until analysis. The pulp and seeds were separated from the peel, frozen, and lyophilized (LH Leybold, Lyovac GT2, Frenkendorf, Switzerland). Subsequently, the lyophilized material was grounded in a laboratory grinder, mixed to obtain homogeneous samples and stored at 4 °C, protected from light, until further analysis.

2.2. Extraction procedures

Ultrasound-assisted extraction was performed using the Bandelin Sonorex Digiplus DL 255 H ultrasound bath. Approximately 0.6 g of plant material was added to Erlenmeyer flasks along with 20 mL of solvent for each of the tests. The extraction parameters were varied (Table 1) across 24 different tests, adjusting extraction time (min), ethanol concentration in the solvent (%), and ultrasonic bath power (%). After extraction and filtration using Whatman No. 4 paper, the solvent was removed using a centrifuge concentrator (Eppendorf, Vienna, Austria) at 30 °C.

To compare with the extracts obtained through ultrasound-assisted extraction, we prepared an extract using classical solid-liquid extraction. Approximately 0.6 g of ground horned melon peel was soaked in 20 mL of 70% ethanol and extracted at room temperature on a magnetic stirrer (Velp Scientifica Magnetic Stirrer) for 24 hours. After filtration using Whatman No. 4 paper, the liquid extract was evaporated to dryness using centrifuge concentrator (Eppendorf, Vienna, Austria) at 30 °C. All extracts (25 in total) were stored at 4 °Cuntil further analysis.

2.3. Total phenolic content

The total phenolic content was determined using the previously described method with some modifications [17]. Extracts were dissolved in a 70% ethanol solution to a final concentration of 10 mg/mL. A sample solution (20 μL) was mixed with diluted Folin–Ciocalteu reagent (100 μL, 1:9, v/v) and shaken vigorously in the microtiter plate. After 3 min, Na_2CO_3 solution (80 μL, 1%) was added, and the mixture was incubated for 2 hours at room temperature. The sample absorbance was measured at 760 nm on a Multiskan™ FC Microplate Photometer, Thermo Scientific™. The total phenolic content was expressed as milligrams of gallic acid equivalents per gram of extract (mg GAE/g extract). The calibration curve was constructed by the serial dilutions of gallic acid using the same protocol. All the extracts were tested in triplicate.

Table 1
Effect of different extraction parameters on the yield and total phenolic content.

Extract Number	EtOH (%)	power (%)	time (min)	yield (%)	TPC mg GAE/100 g of extract
0	/	/	24h	26.71	507.72 ± 44.12
1	50	40	30	43.98	259.66 ± 12.95
2	70	40	30	34.53	283.42 ± 16.81
3	50	60	30	35.15	225.99 ± 40.44
4	70	60	30	35.36	288.37 ± 16.89
5	50	80	30	40.53	236.88 ± 11.25
6	70	80	30	28.32	214.10 ± 18.87
7	50	40	10	26.47	350.27 ± 6.30
8	70	40	10	26.58	315.11 ± 9.08
9	50	40	20	27.33	217.07 ± 13.40
10	70	40	20	27.09	302.24 ± 1.72
11	50	60	10	32.93	247.77 ± 7.86
12	70	60	10	26.37	227.97 ± 38.20
13	50	60	20	34.61	256.68 ± 10.71
14	70	60	20	32.54	297.29 ± 10.43
15	50	80	10	38.30	216.08 ± 6.18
16	70	80	10	32.57	298.28 ± 12.95
17	50	80	20	37.20	256.68 ± 11.88
18	70	80	20	28.66	326.50 ± 69.32
19	50	40	5	37.19	261.64 ± 6.18
20	70	40	5	29.77	282.43 ± 9.55
21	**50**	**60**	**5**	41.99	262.63 ± 50.42
22	70	60	5	35.95	330.96 ± 17.83
23	50	80	5	37.56	225.49 ± 60.92
24	70	80	5	32.04	405.23 ± 130.25

2.4. UHPLC-QToF-MS analysis

The chemical analysis of compounds in the extracts was performed as previously described [18] using an Agilent 1290 Infinity UHPLC system coupled with a 6530C Q-ToF-MS. Extracts were dissolved in methanol to a concentration of 10 mg/mL. Separation was achieved on a Zorbax C18 column (2.1 × 50 mm, 1.8 μm) at 40 °C, with a gradient elution system consisting of acetonitrile and 0.1% formic acid in ultrapure water, operating at a flow rate of 0.3 mL/min and an injection volume of 5 μL.

The QToF-MS system, equipped with an electrospray ionization (ESI) source, operated in both positive and negative ionization modes. Organic acids, phenolic acids, and their derivatives were confirmed primarily in negative ionization mode using Auto MS/MS acquisition (m/z = 100–1500) with a collision energy of 30 eV. Key ESI parameters included a nebulizer pressure of 45 psi, drying gas at 225 °C and 8 L/min, sheath gas at 300 °C and 10 L/min, and a capillary voltage of 2500 V.

Compound identification relied on chromatographic behavior, MS and MS^2 spectra, and literature data comparisons, with molecular formulas and structures determined via high-resolution MS^2 fragmentation. SciFinder (https://scifinder-n.cas.org/) was used to cross-reference the findings, and total ion currents (TICs) were analyzed to identify the most abundant compounds in the extracts.

To differentiate between samples, hierarchical cluster analysis (HCA) plots were constructed using Morpheus software by the Broad Institute (https://software.broadinstitute.org/morpheus/), based on the Spearman method of cluster agglomeration, employing the average linkage method.

2.5. Antibacterial microdilution method

Bacterial species (*P. aeruginosa*, PAO1 strain) were cultured overnight at 37 °C in Tryptic soy broth (TSB) medium. The bacterial cell suspension was adjusted with sterile saline to a concentration of 10^6 units in a final volume of 100 μL per well containing the solution of tested extracts. Minimum inhibitory concentrations (MICs) and minimum bactericidal concentrations (MBCs) were determined by a serial dilution technique using 96-well microtitre plates with the solutions of tested compounds (0.125–16 mg/mL) according to previous protocols [19]. The blank sample contained only TSB solution, while negative control contained TSB and bacteria cell suspension. Streptomycin (SigmaAldrich, Germany) was used as a positive control.

2.6. Molecular docking

Molecular docking is a useful method that can show how molecules bind to proteins [20,21], and also how the bond is formed, for example protein-peptide, like in the prevously described work [22], and for strategic targeting virus proteins [23].

Molecular docking was done according to a similar principle but with different programs as in the previously reported procedure [24]. Canonical SMILES of the tested ligands are imported from SciFinder (https://scifinder-n.cas.org/) or created by the online software SMILES generator from cheminfo.org. First, the .txt file containing canonical SMILES and names of the compound was loaded into the YASARA program [25] Version 23.9.29 and the file was converted in the .sdf format without energy minimization. In YASARA, only the adding of hydrogens was performed. Molecular docking was carried out using the MzDock program [26]. First, the ligands energies were minimized using the MMFF94 force field at a pH of 7.4. Enzyme elastase B was prepared by first ploading the .pdb file (LasB, PDB: 8CC4) of the enzyme, followed by extraction of enzyme chain A, addition of the hydrogens, energy minimization using the Kollman charges option, removal of the solvent (water) and preservation of the ions. The binding site of the tested ligands was defined by the co-crystalised ligands. Lipase A (LipA, PDB: 1EX9) was prepared using the same procedure, except for chain extraction. Imaging of the enzyme and the binding site of the enzyme was created using the CCP4MG program [27]. Obtained .pdbqt files from the MZDock were converted into the .pdb files via ChimeraX program [28], and the 2D plots of the ligand interaction with the amino acids were created by the BIOVIA Discovery Studio v24.1.0.23.298 (Dassault Systèmes Biovia Software Inc., 2012). Site-specific molecular docking was performed. The active site of the enzyme is based on a previously co-crystallized ligand with the enzyme from the PDB database. Ligands that had a lower binding energy expressed in kcal/mol were considered the ligand that binds more strongly to the active site.

3. Results and discussion

3.1. Extractions, yields and TPC

Ultrasonic-assisted extraction (UAE) is considered a green extraction technique because it offers several advantages over traditional methods. Due to its high efficiency, which is achieved by reducing the amount of solvent and extraction time, it is more economical and environmentally friendly. Additionally, use of lower temperatures in UAE reduces the possibility of thermal degradation and is especially well-suited for extracting thermo-sensitive chemicals. All these characteristics suggest that ultrasound-assisted extraction is an efficient and sustainable method, with potential applications across various fields, including the study of natural products [29].

The extraction conditions, yield of extracts, and their total phenolic contents (TPCs) are presented in Table 1. Considering ethanol concentration, the results showed that higher ethanol concentrations (70%) do not always lead to higher yields compared to lower concentrations (50%). This can be observed by comparing extract 1 (50% EtOH) and extract 2 (70% EtOH), which differ only in ethanol concentration. Despite the higher ethanol concentration in extract 2, it did not result in a higher yield. This suggests that solvent concentration can significantly impact the overall extract yield, with moderate concentrations (50%) outperforming higher concentrations (70%), in our samples. As for the influence of UAE power, it can generally be noted that higher power settings (e.g. 80%) result in higher yields. This was observed in extract 5 (50% EtOH, 80% power, 30 min) and extract 21 (50% EtOH, 60% power, 5 min), which both had yield over 37%. However, in extract 6 (70% EtOH, 80% power, 30 min), the yield was lower, demonstrating that other factors, such as ethanol concentration and extraction time, can outweigh the benefits of higher power. Extracts with shorter extraction times (e.g., 5 min) often yield moderate amounts of extract, with notable exceptions like extract 21 (50% EtOH, 60% power, 5 min) that had a yield of 41.99%. Overall, it can be observed that longer extraction time (e.g., 30 min) typically provide higher yield, and this often reflected in higher phenolic content as well. For example, extract 4 (70% EtOH, 60% power, 30 min) with a yield of 35.36% and a phenolic content of 288.37 mg GAE/100 g extract. This can be associated with longer time of extraction, which enables more thorough extraction of the phenolic compounds. However, there may be deviation from this trend. For example, in case of extract 24 (70% EtOH, 80% power, 5 min), despite the short extraction time, extract had a comparatively moderate yield (32.04%), but the highest TPC (405.23 mg GAE/100 g extract). Conversely, extracts with lower phenolic content, such as extract 5 (50% EtOH, 80% power, 30 min), had a relatively high yield (40.53%), but the TPC was only 236.88 mg GAE/100 g extract. This implies that, in addition to maximizing yield, the concentration of bioactive substances such as phenolic compounds, needs to be optimized by adjusting extraction time and ethanol concentration. Furthermore, the obtained data suggested that the yield and the phenolic content of the extracts are not always directly correlated. For instance, phenolics are present in lower concentrations in extracts with higher yields, like extract 1 (50% EtOH, 40% power, 30 min) which yielded 43.98%, than in extracts with lower yields, such as extract 24 (70% EtOH, 80% power, 5 min) which had a yield of 32.04%, also contained 405.23 mg GAE/100 g extract.

This demonstrates the complexity of the extraction process and how higher yield does not necessarily correlate with increased TPC.

Regarding previously published data on TPC identified in kiwano, our literature survey showed that obtained values are in accordance with those reported by Ezekaibeya et al. (2020); the authors have reported TPC to be 1.54 ± 0.13 mg/g for horned melon peel [30].

Overall, this study is the first to systematically explore the effects of various ultrasound-assisted extraction (UAE) parameters on the extraction yield and total phenolic content (TPC) of horned melon peel extracts. While UAE has been widely applied to other plant matrices, its application to horned melon peel, a largely underutilized by-product of fruit processing, has not been previously documented. By filling this gap in literature, our research clarifies the metabolite makeup of horned melon peel, a resource that has not yet been well studied in science.

3.2. Phytochemical composition of *C. metuliferus*

Phytochemical composition of *C. metuliferus* peel was analyzed using UHPLC-QToF-MS, revealing molecular diversity of bioactive compounds. The analysis of identified phenolic acids, as well as other metabolites, contribute to the understanding of its biological potential. Table 2 provides comprehensive details about the different compounds detected in an extract, such as their masses, retention times, HRMS data, and molecular formulas. These substances encompass a broad spectrum of chemical classes, such as phenolic and organic acids, and derivatives of benzoic acid. Benzoic acid derivatives make up for the majority of the compounds in the table, including 2,5-dihydroxybenzoic acid 5-*O*-pentosyl-pentoside ($[M–H]^-$ at *m/z* 417), vanillic acid 4-*O*-hexoside ($[M–H]^-$ at *m/z* 329), and 3,4,5-trihydroxybenzoic acid 3-*O*-pentoside ($[M–H]^-$ at *m/z* 301). As for the bioactive properties of the identified compounds, benzoic acid and its derivatives are frequently employed as flavoring agents and antibacterial and antifungal preservatives in various industries, including food, cosmetic and pharmaceutical [31]. Furthermore, vanillic acid and its derivatives are known for antioxidant activity, which has immense importance in protecting cells from inflammation and oxidative stress—key mechanisms underlying their demonstrated anticancer, antidiabetic, and antiulcer properties [32]. Among the other identified compounds, the presence of the iridoid glycoside catalpol ($[M–H]^-$ at *m/z* 361) is particularly noteworthy, as it has been linked to various biological properties, including anti-inflammatory, antioxidant, and neuroprotective [33]. The presence of more complex compounds, such as vanillic acid 4-*O*-hexosyl-hexoside ($[M–H]^-$ at *m/z* 491) and vanillic acid 4-*O*-rhamnosy-hexoside ($[M–H]^-$ at *m/z* 475), which contain multiple sugar moieties, indicates the extract's potential as a source of glycosylated compounds.

The heatmap (Fig. 1) demonstrates clustering of the horned melon peel extracts based on their metabolite profiles, with groupings that reflect similarities in their chemical composition. The clusters highlighted variations in the intensity of specific compounds as influenced by UAE parameters. The data revealed clear trends linking extraction parameters to the metabolite profiles. Higher ethanol concentrations (70%) generally enhance the extraction of identified compounds. Extracts 2, 4, 8, and 10 (70% ethanol) showed higher relative abundances of compounds like vanillic acid derivatives and hydroxybenzoic acid

Table 2
Compound names, retention times (tR, min), molecular formulas, MS data (calculated and exact masses, as well as mean mass accuracy – Δ mDa), major MS^2 fragment ions of the compounds present in the hydro-ethanolic peel extracts of *C. metuliferus*.

No	Compound name	t_R, min	Molecular formula, $[M–H]^-$	Calculated mass, $[M–H]^-$	Exact mass, $[M–H]^-$	Δ mDa	MS^2 Fragments, (% Base Peak)
Hydroxybenzoic acids							
1	3,4,5-trihydroxybenzoic acid 3-*O*-pentoside	2.75	$C_{12}H_{13}O_9^-$	301.05600	301.06321	−7.21	125.02486(86), 151.00193(9), **168.00713**(100), 169.01187(17), 283.04718(5)
2	Vanillic acid 4-*O*-hexoside	3.23	$C_{14}H_{17}O_9^-$	329.08781	329.09013	−2.33	**108.02171**(100), 123.04551(41), 152.01152 (70), 167.03555(37)
3	2-hydroxybenzoic acid 4-*O*-pentoside	5.06	$C_{12}H_{13}O_8^-$	285.06159	285.06460	−3.01	**108.02274**(100), 109.02803(22), 152.01228 (47), 153.01752(9)
4	Vanillic acid 4-*O*-hexosyl-hexoside	5.38	$C_{20}H_{27}O_{14}^-$	491.14010	491.14501	−4.91	101.02447(5), 123.04538(16), 152.01093(4), **167.03579**(100), 168.03833(11), 209.04425(5)
5	3,4-dihydroxybenzoic acid	5.65	$C_7H_5O_4^-$	153.01933	153.02107	−1.74	107.01240(3), 108.02065(9), **109.03010**(100), 110.03119(8), 135.00921(20)
6	Vanillic acid 4-*O*-rhamnosy-hexoside	5.59	$C_{20}H_{27}O_{13}^-$	475.14572	475.14683	−1.11	108.02239(5), 123.04508(7), 152.01183(23), 153.01757(6), **167.03580**(100), 168.03858(11)
7	Hydroxybenzoic acid 2-*O*-hexoside	5.92	$C_{13}H_{15}O_8^-$	299.07670	299.08182	−5.12	**137.02495**(100), 138.02803(10)
8	2,5-dihydroxybenzoic acid 5-*O*-pentosyl-pentoside	6.26	$C_{17}H_{21}O_{12}^-$	417.10330	417.10873	−5.43	109.02963(23), **152.01231**(100), 153.01662(12)
9	4-hydroxybenzoic acid	8.28	$C_7H_5O_3^-$	137.02442	137.02553	−1.11	NA
Other Compounds							
10	Homocitric acid	1.61	$C_7H_9O_7^-$	205.03538	205.03737	−1.99	**111.00918**(100), 112.01332(8)
11	Citric acid	1.74	$C_6H_7O_7^-$	191.01973	191.02131	−1.59	**111.00937**(100), 112.00996(5)
12	Catalpol	2.68	$C_{15}H_{21}O_{10}^-$	361.11402	361.11682	−2.80	101.02385(23), 135.04605(79), 138.03712(28), **153.05576**(100), 164.07265(54)
13	1,5-Dimethylcitric acid	4.16	$C_8H_{11}O_7^-$	219.05103	219.05259	−1.57	**111.00917**(100), 112.01165(6)
14	Phenyllactic acid 2-*O*-hexoside	6.06	$C_{15}H_{19}O_8^-$	327.10854	327.10941	−0.87	121.06582(19), 147.04431(4), **165.05603**(100)
15	Phenylethyl hexosyl-hexoside	6.40	$C_{20}H_{29}O_{11}^-$	445.17154	445.17590	−4.36	101.02491(54), 113.02479(40), 119.03555(35), 175.11337(72), 201.09274(62), **219.10317**(100)
16	Vanilloloside	6.46	$C_{14}H_{19}O_8^-$	315.10800	315.11036	−2.36	101.02127(16), 111.00254(12), 121.00283(16), **130.08662**(100), 134.03892(11), 143.11906(59)
17	Decaffeoyl-acteoside	6.60	$C_{20}H_{29}O_{12}^-$	461.16645	461.17038	−3.93	101.02920(20), 146.03706(21), 161.03976(22), 167.03610(37), **179.07051**(100), 209.04625(27)
18	4-hydroxymethyl-phenyl 1-*O*-hexosyl-hexoside	6.74	$C_{19}H_{27}O_{12}^-$	447.15030	447.15564	−5.34	**101.02488**(100), 113.02468(43), 131.03523 (34), 161.04623(42), 269.10405(54), 401.14717 (20)
19	Benzyl pentosyl-hexoside	6.93	$C_{18}H_{25}O_{10}^-$	401.14532	401.14914	−3.82	**101.02327**(100), 113.02780(74), 161.04226 (27), 175.03692(26), 193.06073(30), 195.06347 (15)
20	8-hydroxy-2,7-dimethyl-deca-2,4-dienedioic acid 8-*O*-hexoside	7.68	$C_{18}H_{27}O_{10}^-$	403.16040	403.16524	−4.84	101.02480(40), 113.02455(34), 119.03463(17), 135.11791(20), 161.09717(10), **179.10832**(100)

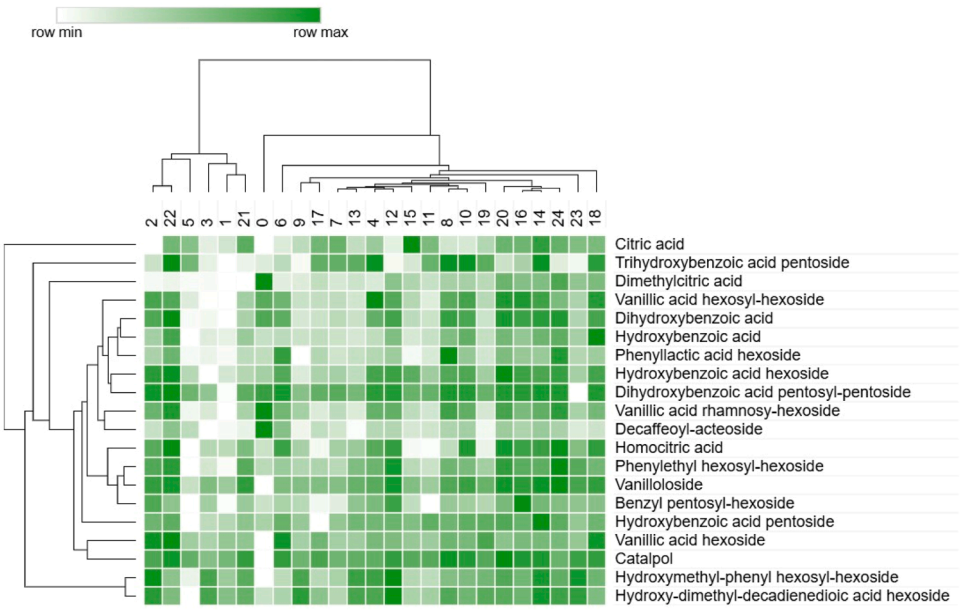

Fig. 1. Hierarchical cluster analysis of molecular diversity in horned melon peel extracts based on extraction parameters.

compared to extracts obtained using 50% ethanol (e.g., extracts 1, 3, 7, and 9). This suggests that ethanol's polarity plays a critical role in solubilizing metabolites from the peel matrix. Regarding ultrasonic power, higher power levels (80%) correlated with greater extraction yields of bioactive compounds. Extracts 4, 12, 20, 22 (80% power) exhibit pronounced signals for hydroxybenzoic acid hexoside and dihydroxybenzoic acid pentosyl-pentoside compared to extracts obtained at lower power (40%, e.g., extracts 1, 3, 5, 9). This effect is likely due to increased cell wall disruption and improved solvent penetration at higher ultrasonic intensities. Extraction time played a dual role. Longer durations (30 min) do not necessarily always result in higher yields of certain compounds, as seen in samples 1, 3, and 5, where key compounds like hydroxybenzoic acid and vanillic acid hexoside were not prominent. Conversely, even short durations (5 min) produced measurable metabolite content when combined with optimal ethanol concentration and high power, as observed in samples 20–24. This demonstrates that UAE can be highly efficient, even with minimal extraction times, provided the other parameters are optimized. Extract 0 (control, 24-hour maceration) was significantly different than UAE-treated samples. While maceration yielded a basic chemical profile, UAE enhanced the abundance and diversity of metabolites—even at shorter times, as seen in extracts 20–24. Using 70% ethanol, high ultrasonic power (80%), and moderate extraction times (10–30 min) proved to be an effective approach for obtaining a rich and diverse chemical profiles from horned melon peels. This demonstrates the potential of UAE as a time-efficient and targeted method for extracting specific bioactive compounds.

Data in Supplementary Table S1 presents the highest relative abundances of compounds in *C. metuliferus* peel extracts, reflecting their distribution at different extraction conditions as measured by total ion current (TIC). These findings support selective distribution of compounds under particular extraction conditions, offering a deeper insight into the influence of extraction parameters on the phytochemical recovery. For instance, 3,4-dihydroxybenzoic acid, vanillic acid 4-*O*-hexoside, 2,5-dihydroxybenzoic acid 5-*O*-pentosyl-pentoside, homocitric acid, and 3,4,5-trihydroxybenzoic acid 3-*O*-pentoside were found in high concentrations in extract 22, making it the sample with the highest number of identified compounds and the highest relative abundances. Extract 0 contained compounds such as vanillic acid 4-*O*-rhamnosyl-hexoside, 1,5-dimethylcitric acid, and decaffeoyl-acteoside in the highest proportions, suggesting that traditional extraction method is particularly effective for these bioactive molecules. Similarly, extract 4 demonstrated prevalence of vanillic acid 4-*O*-hexosyl-hexoside, indicating that the stability or solubility of this chemical was optimal under those conditions (Table 1). Extracts 8 and 18 had higher level of phenyllactic acid 2-*O*-hexoside and 4-hydroxybenzoic acid, respectively. Benzyl pentosyl-hexoside, citric acid, and 2-hydroxybenzoic acid 5-*O*-pentoside were the most common compounds in extracts 16, 15, and 14, respectively, highlighting the effectiveness of the applied conditions for recovering specific metabolites. Extract 12 contained high share of hexosides, including 4-hydroxymethyl-phenyl 1-*O*-hexosyl-hexoside and 8-hydroxy-2,7-dimethyl-deca-2,4-dienedioic acid 8-*O*-hexoside. This group of complex glycosides was also abundant in other tested extracts. For example, vanillic acid 4-*O*-rhamnosy-hexoside, 1,5-dimethylcitric acid, and decaffeoyl-acteoside were present in extract 0, phenylethyl hexosyl-hexoside and vanilloloside in extract 24, and hydroxybenzoic acid 2-*O*-hexoside and catalpol in extract 20.

This study demonstrated that solvent polarity, extraction time, and temperature represent key factors influencing composition of obtained extracts. Furthermore, it has been shown that specificity of the extraction process is evident in all samples, each displaying distinct chemical profiles, implying that the applied parameters were optimal. Our literature review confirms that this is the first study that investigated phytochemical composition and bioactive properties of *C. metuliferus* peel in such a comprehensive manner. Furthermore, our findings provided the first insights into the chemical diversity and bioactive properties of extracts obtained through targeted extraction procedures, with some extracts showing remarkable capacity to concentrate a variety of phytochemicals. These results offer valuable informations for the potential use of *C. metuliferus* peel in medicinal, nutraceutical, and functional applications.

3.3. Antibacterial evaluation

Result of bactericidal, bacteriostatic and inhibitory activity of different molecules or extract against *P. aeruginosa* were previously reported [34]. The obtained results of antimicrobial activity of extracts against resistant *P. aeruginosa* strain are presented in Table 3. The range of MIC values variated from as low as 0.25 mg/mL to as high as 2 mg/mL, with most extracts showing MIC values of 0.5 mg/mL. This indicated that the majority of extracts demonstrated antimicrobial activity at relatively low concentrations. Extract 0 exhibited the highest

Table 3
Minimum inhibitory concentration (MIC) and minimum bactericidal concentration (MBC) of the tested hydro-ethanolic extracts of *C. metuliferus* peel.

Extract number	MIC (mg/mL)	MBC (mg/mL)
0	2	4
1	0.5	1
2	0.5	1
3	0.5	1
4	0.5	1
5	0.5	1
6	0.5	1
7	1	2
8	0.5	1
9	0.5	1
10	0.5	1
11	0.5	1
12	0.5	1
14	0.5	1
15	0.5	1
16	0.5	1
17	0.5	1
18	0.25	0.5
19	0.25	0.5
20	0.25	0.5
21	0.25	0.5
22	0.5	1
23	0.5	1
24	0.5	1
Str*	0.025	0.05

* Str- streptomycin.

MIC value of 2 mg/mL, indicating that classical solid-liquid extraction is not effective in extracting compounds with antibacterial properties, despite the fact that this extract showed the highest content of total phenolics. This could possibly be ascribed to the different type of interactions between the compounds present in the extract, or their relative abundance. Contrary to extract 0, extracts 18–21 showed the best antimicrobial potential with MIC 0.25 mg/mL, which implies that the compounds abundant in these extracts are responsible for good antibacterial activity. As for the bactericidal activity, our results indicated MBC values range from 0.5 mg/mL to 4 mg/mL. Again, as was the case with MIC values, extracts 18–21 showed the most promising results, with MBC values as low as 0.5 mg/mL. These antibacterial properties can be attributed to the synergistic effects of varying concentrations of identified compounds present in the extracts, as shown in Table 2. Literature survey showed that antimicrobial and antiviral activity of *C. metuliferus* has been demonstrated previously by several authors [35–37]. For instance, Šovljanski et al. (2022) [37], reported that the peel has the highest antimicrobial potential (inhibition zones ranging from 23 to 37 mm) towards pathogenic bacteria *Bacillus cereus* and *P. aeruginosa*, as well as fungi such as *Aspergillus brasiliensis*, and *Penicillium aurantiogriseum*. The pulp extract was especially active against *Salmonella typhimurium*, while the seed extract inhibited yeasts *Saccharomyces cerevisiae* and *Candida albicans*. Similar antimicrobial potential was also achieved for *S. gallinarum*, but with methanolic extract (MIC 50 mg/mL), while the water extract showed an inhibition zone of 7.50 ± 0.55 mm at 600 mg/mL. In contrast, *n*-hexane and chloroform extracts were ineffective [35]. The activity of horned melon peel extracts against *P. aeruginosa*, as reported by Šovljanski et al. (2022) [37], was weaker, with MIC value of 3.125 mg/mL compared to 0.25 mg/mL for our extract. All the presented results indicate that the level of activity mainly depends on the type of extract, highlighting the importance of selecting suitable solvents and extraction methods to maximize the efficacy of bioactive compounds against pathogenic microorganisms.

The increasing difficulty in managing infections due to rising antibiotic resistance has highlighted the need for alternative approaches in treatment [38]. Treating *P. aeruginosa* infections, particularly in cystic fibrosis patients, remains challenging due to bacterium's ability to persist despite treatment and its rapid adaptation through mechanisms like altered outer membrane permeability, influenced by lipopolysaccharides (LPS) and porin proteins [39]. Molecular docking has become a crucial tool in this effort, enabling the identification of therapeutic targets by focusing on interactions between pathogenic microorganisms and specific proteins. Recent advancements in software have significantly accelerated the process, allowing quicker and more cost-effective analysis of enzyme interactions, resistance mechanisms, and virulence factors, thus facilitating faster drug development [38]. Molecular docking is used for screening of protein-molecule interaction, before experimental conformation [40].

This study provided for the first time optimization of the ultrasound-assisted extraction (UAE) parameters for horned melon peel, achieving superior antibacterial activity (MIC as low as 0.25 mg/mL) against a resistant *Pseudomonas aeruginosa* strain. It also uniquely demonstrated that classical solid-liquid extraction, despite yielding high phenolic content, is less effective-emphasizing the critical role of optimized extraction methods in maximizing bioactivity.

3.4. Molecular docking

Molecular docking studies were conducted for all 20 identified compounds in the peel of kiwano to reveal their potential interactions with key virulence factors of *P. aeruginosa*, namely elastase B and lipase A, which have crucial roles in the pathogenicity of the bacterium [41]. Elastase from *P. aeruginosa* serves as an extracellular virulence factor that improves the pathogenicity of the bacteria, while porcine pancreatic elastase (PPE) serves more for digestion [42,43]. Porcine pancreatic elastase is used as protein for molecular docking in prevoius work [44, 45]. Unlike PPE, elastase B from *P. aeruginosa* have different structure, with two chains, and with the weight of 67.24 kDa.

Using *in silico* tools, the simulation of binding of each identified compound to these enzymes was conducted, leading to potential inhibition of their activity, thereby reducing *P. aeruginosa* host invasion and facilitating its eradication. This approach enables the prediction of the binding affinity and interaction dynamics between the bioactive compounds and the target enzymes, providing insights into their potential as therapeutic agents against bacterial infections.

The docking scores of each ligand, calculated as the binding affinity (kcal/mol) for each target enzyme, are presented in Fig. 2. Our results showed that all the selected compounds from hydro-ethanolic extracts of *C. metuliferus* fruit exocarp bind to the two tested enzymes. The strongest interactions with elastase B were observed for compounds with high negative affinity values, such as decaffeoyl-acteoside (−10.4 kcal/mol), vanillic acid 4-*O*-rhamnosy-hexoside (−9.3 kcal/mol), vanillic acid 4-*O*-hexosyl-hexoside (−9.0 kcal/mol) and benzyl pentosyl-hexoside (−9.0 kcal/mol). This implies that these compounds might serve as strong modulators or inhibitors of elastase B activity. These substances also exhibited comparatively high binding affinities with lipase A: decaffeoyl-acteoside (−8.9 kcal/mol), vanillic acid 4-*O*-rhamnosy-hexoside (−8.5 kcal/mol), and vanillic acid 4-*O*-hexosyl-hexoside (−8.2 kcal/mol) making them potent lipase A modulators or inhibitors. Derivates of hydroxybenzoic acid with solid binding affinities for elastase B, including 3.4.5 trihydroxybenzoic acid 3-*O*-pentoside (−8.1 kcal/mol) and 2-hydroxy benzoic acid 5-*O*-pentoside (−8.1 kcal/mol), were somewhat weaker against lipase A, with affinity values of −7.7 kcal/mol and −7.2 kcal/mol, respectively. Both citric and homocitric acids exhibited relatively lower binding affinities for both targets (−6.3 kcal/mol for elastase B and −5.5 kcal/mol for lipase A; and −6.7 kcal/mol for elastase B and −5.5 kcal/mol for lipase A, respectively). Elastase B exhibited moderate to strong binding to phenyllactic acid derivatives such as phenyllactic acid 2-*O*-hexoside and phenylethyl hexosyl-hexoside (affinities of −7.9 kcal/mol and −8.2 kcal/mol, respectively), while lipase A exhibited weaker binding (affinities of −6.9 kcal/mol and −7.9 kcal/mol, respectively). Decaffeoyl-acteoside showed an affinity of −10.4 kcal/mol for elastase B and −8.9 kcal/mol for lipase A making it a promising candidate for further research in therapeutic

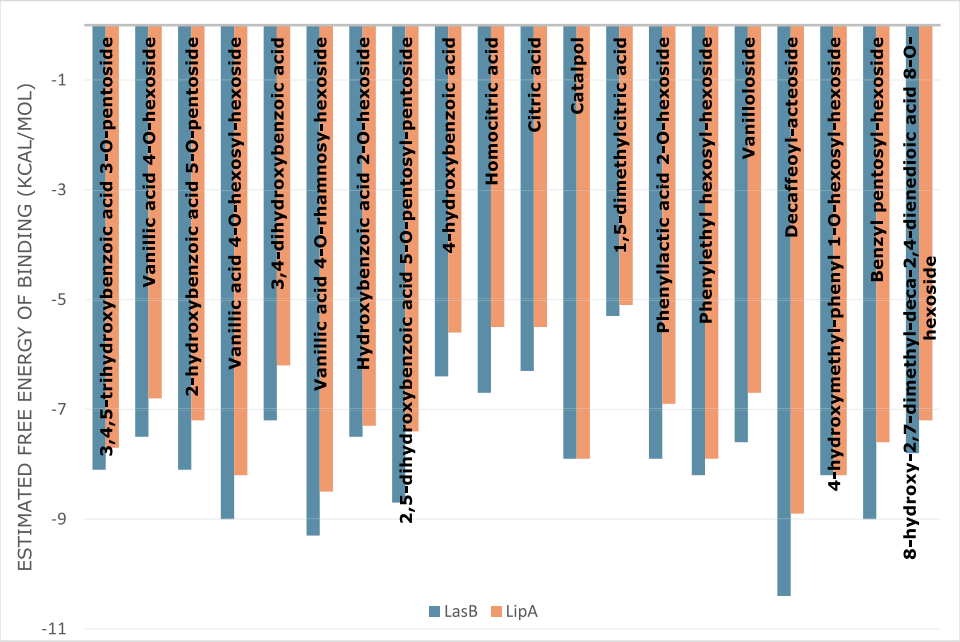

Fig. 2. Estimated free energy of binding (kcal/mol) for *C. metuliferus* peel compounds interacting with elastase B (LasB) and lipase A (LipA).

applications targeting both enzymes (Figs. 3 and 4), based on the observed high affinities.

In case of elastase B from *P. aeruginosa*, the binding site was established using the co-crystalized phosphonic based inhibitor. The strongest binding was observed with decaffeoyl-acteoside (binding energy of −10.7 kcal/mol), compared to the other tested compounds. Among all amino acids in the binding site presented in Fig. 2, only few of the amino acids were directly responsible for decaffeoyl-acteoside binding: 153Leu, 155Tyr, 115Trp, 144His, 140His, 112Asn, 113Ala, 137Val and 198Arg from chain A. Oxygens from the petide bond originated from the 137Val and 115Ala formed conventional hydrogen bonds with hydroxyl groups from both the sugar and non-sugar moieties of decaffeoyl-acteoside. Additionally, Asn112 and Arg198 residues were also involved in conventional hydrogen bonding with the ligand. Unfavorable donor-donor and acceptor-acceptor hydrogen bonds were observed between the 115Trp and 144His. Other interaction, such as π-sigma, π-π stacked, and alkyl-alkyl interactions, occurred between 140His, 155Tyr, and 137Val. Decaffeoyl-acteoside had the best affinity binding among all tested compounds as well as in the case of extracellular enzyme lipase A from *P. aeruginosa*. Among the amino acid residues in the lipase A

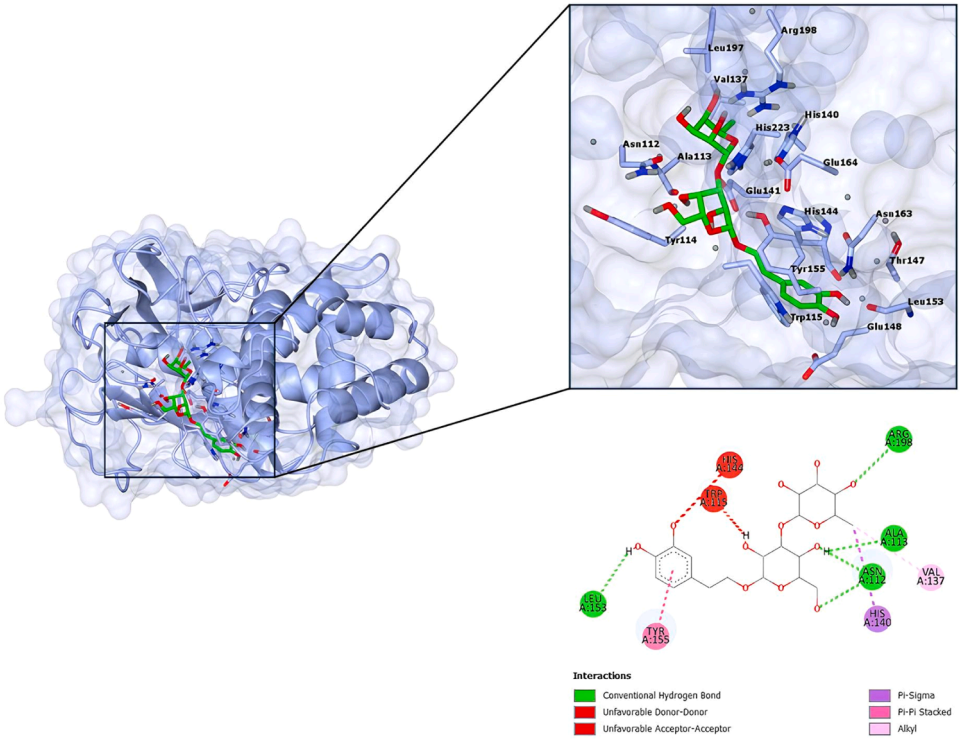

Fig. 3. LasB (Elastase B, PDB:8CC4), amino acids in binding site of the ezyme, 2D plot of the amino acid that correspond to the ligand (decaffeoyl-acteoside).

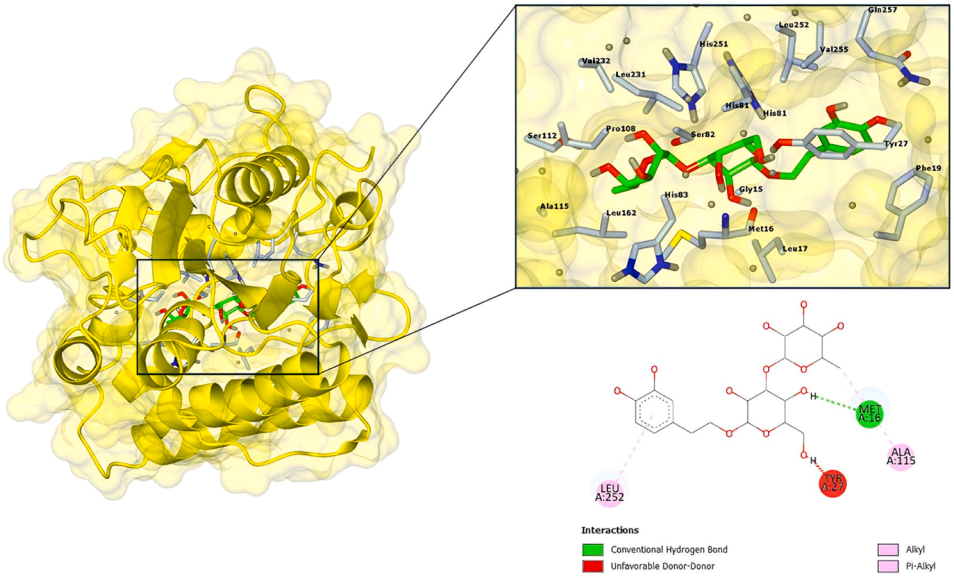

Fig. 4. LipA (Lipase A, PDB:1EX9, aminoacids in binding site of the ezyme, 2D plot of the amino acid that correspond to the ligand (decaffeoyl-acteoside).

binding site, only a few were actively involved in ligand binding. Oxygen from the peptide bond originated from the 16Met formed a hydrogen bond with the hydroxyl group of hexose sugar moiety of tested compound, while an unconventional hydrogen bond was formed between the same hexose part and the hydroxyl group from the amino acid residue from 27Tyr. Alkyl and π-alkyl interactions were observed between the 115Ala and 252Leu, respectively.

This study is the first to explore the potential of bioactive compounds from *C. metuliferus* peel as inhibitors of key virulence factors in *Pseudomonas aeruginosa* - elastase B and lipase A - using molecular docking. For the first time, the binding affinities of 20 identified compounds were systematically evaluated and supported by detailed analyses of binding sites and interaction mechanisms. Our results provide novel insights into the therapeutic potential of *C. metuliferus* peel metabolites in combating bacterial infections by targeting virulence factors. As we demonstrated in this study, kiwano, a neglected crop, has considerable potential as a source of bioactive compounds with therapeutic properties. The tested extracts contained a variety of phytochemicals that could be further explored in development of therapies targeted towards virulence factors of *P. aeruginosa*. Further research into the specific bioactive profile of kiwano is essential to fully understand its medicinal potential. This would not only help in combating infections like those caused by *P. aeruginosa* but also promote sustainability by valorizing parts of the plant typically discarded.

4. Conclusion

This is the first study that evaluated the impact of various UAE parameters on extraction yield and total phenolic content (TPC) of horned melon peel extracts in such a comprehensive manner. Furthermore, for the first time, the detailed phytochemical profile of *C. metuliferus* peel using UHPLC-QToF-MS was presented, uncovering a diverse array of bioactive compounds, including phenolic acids, organic acids, and glycosylated derivatives-and highlighting the influence of extraction conditions on the selective enrichment of these metabolites. Our investigation of antimicrobial properties of C. metuliferus extract revealed its potential as an alternative therapeutic agent, especially towards *P. aeruginosa*, with the lowest MIC and MBC values observed in extracts 18–21. Molecular docking analysis of the bioactive compounds present in the extract revealed that certain compounds, such as decaffeoyl-acteoside, vanillic acid derivatives, and benzyl pentosyl-hexoside, bind strongly to the virulence factors elastase B and lipase A. Decaffeoyl-acteoside emerged as a particularly promising compound, demonstrating strong interactions with both enzymes, making it a candidate for further research and therapeutic development. However, further studies are required to validate the efficacy and safety of these extracts for therapeutic use. The pharmacokinetics of potential therapeutics should also be investigated, based on the model previously established, which included both sexes [46]. This study emphasizes the importance of plant-based compounds as a promising source of new antimicrobial agents, highlighting their potential in mitigating the growing challenge of antibiotic resistance.

Funding

This work has been supported by Ministry of Science, Technological Development and Innovations of the Republic of Serbia (451–03–66/2024–01/200007, 451–03–66/2024–03/200178, 451–03–65/2024–03/200178 and 451–03–66/2024–03/200168).

CRediT authorship contribution statement

Mladen Rajaković: Writing – original draft, Methodology, Investigation, Formal analysis, Conceptualization. **Uroš Gašić:** Validation, Investigation, Funding acquisition. **Danka Bukvički:** Writing – review & editing, Investigation. **Mirjana Pešić:** Writing – review & editing, Funding acquisition, Conceptualization. **Danijel Milinčić:** Validation, Investigation. **Jovana Petrović:** Writing – original draft, Data curation, Conceptualization. **Ivana Sofrenić:** Writing – review & editing, Supervision, Investigation. **Carlos S.H. Shiraishi:** Software, Investigation, Data curation. **Dejan Stojković:** Writing – review & editing, Supervision, Funding acquisition, Conceptualization.

Declaration of competing interest

The authors declare that they have no known competing financial interests or personal relationships that could have appeared to influence the work reported in this paper.

Supplementary materials

Supplementary material associated with this article can be found, in the online version, at doi:10.1016/j.molstruc.2025.142600.

Data availability

Data will be made available on request.

References

[1] N.N. Wannang, N.S. Jimam, S. Omale, M.L.P. Dapar, S.S. Gyang, J.C. Aguiyi, Effects of Cucumis metuliferus (Cucurbitaceae) fruits on enzymes and haematological parameters in albino rats, Afr. J. Biotechnol. 6 (2007) 2515–2518, https://doi.org/10.5897/ajb2007.000-2400.

[2] M. Ajuru, F. Nmom, A review on the economic uses of species of cucurbitaceae and their sustainability in Nigeria, 2 (2017) 17–24.10.11648/j.ajpb.20170201.14.

[3] V. Luchian, G. Teodosiu, Research results regarding the anatomy of some medicinal plants of cucurbitaceae, LXIII (2019) 635–642.

[4] M.F.R. Mallick, M. Masui, Origin, distribution and taxonomy of melons, Sci. Hortic. 28 (1986) 251–261, https://doi.org/10.1016/0304-4238(86)90007-5.

[5] Cancer Biology 2015;5(1) http://www.cancerbio.net Uses of, 5 (2015) 24–34.

[6] D.C. Manjunathagowda, M. Pitchaimuthu, V. Hiremata, G.C. Sathisha, S. Soni, M. V. Dhananjaya, D.C. Lakshmana Reddy, Horny gourd (Cucumis metuliferus L.): a hidden vegetable boon for human nutrition, Genet. Resour. Crop. Evol. 70 (2023) 1903–1911, https://doi.org/10.1007/s10722-023-01601-z.

[7] G. Singh, M.A. Hossain, D. Al-Fahad, V. Gupta, S. Tandon, H. Soni, C. V. Narasimhaji, M. Jaremko, A.H. Emwas, M.J. Anwar, F. Azam, An in-silico approach to target multiple proteins involved in anti-microbial resistance using natural compounds produced by wild mushrooms, Biochem. Biophys. Rep. 40 (2024) 101854, https://doi.org/10.1016/j.bbrep.2024.101854.

[8] C. Yin, M.Z. Alam, J.T. Fallon, W. Huang, Advances in development of novel therapeutic strategies against multi-drug resistant Pseudomonas aeruginosa, Antibiotics 13 (2024), https://doi.org/10.3390/antibiotics13020119.

[9] D. Reynolds, M. Kollef, The epidemiology and pathogenesis and treatment of Pseudomonas aeruginosa infections: an update, Drugs 81 (2021) 2117–2131, https://doi.org/10.1007/s40265-021-01635-6.

[10] A. Kaminski, K.H. Gupta, J.W. Goldufsky, H.W. Lee, V. Gupta, S.H. Shafikhani, Pseudomonas aeruginosa ExoS induces intrinsic apoptosis in target host cells in a manner that is dependent on its GAP domain activity, Sci. Rep. 8 (2018) 1–15, https://doi.org/10.1038/s41598-018-32491-2.

[11] H. Silistre, D. Raoux-Barbot, F. Mancinelli, F. Sangouard, A. Dupin, A. Belyy, V. Deruelle, L. Renault, D. Ladant, L. Touqui, U. Mechold, Prevalence of ExoY activity in Pseudomonas aeruginosa reference panel strains and impact on cytotoxicity in epithelial cells, Front. Microbiol. 12 (2021), https://doi.org/10.3389/fmicb.2021.666097.

[12] A.C.M. Galdino, L. Viganor, A.A. De Castro, E.F.F. Da Cunha, T.P. Mello, L. M. Mattos, M.D. Pereira, M.C. Hunt, M. O'Shaughnessy, O. Howe, M. Devereux, M. McCann, T.C. Ramalho, M.H. Branquinha, A.L.S. Santos, Disarming Pseudomonas aeruginosa virulence by the inhibitory action of 1,10-phenanthroline-5,6-dione-based compounds: elastase B (lasB) as a chemotherapeutic target, Front. Microbiol. 10 (2019) 1–16, https://doi.org/10.3389/fmicb.2019.01701.

[13] M. Nardini, D.A. Lang, K. Liebeton, K.E. Jaeger, B.W. Dijkstra, Crystal structure of Pseudomonas aeruginosa lipase in the open conformation. The prototype for family I.1 of bacterial lipases, J. Biol. Chem. 275 (2000) 31219–31225, https://doi.org/10.1074/jbc.M003903200.

[14] P. Tielen, F. Rosenau, S. Wilhelm, K.E. Jaeger, H.C. Flemming, J. Wingender, Extracellular enzymes affect biofilm formation of mucoid Pseudomonas aeruginosa, Microbiology 156 (2010) 2239–2252, https://doi.org/10.1099/mic.0.037036-0 (N. Y).

[15] P. Tielen, H. Kuhn, F. Rosenau, K.E. Jaeger, H.C. Flemming, J. Wingender, Interaction between extracellular lipase LipA and the polysaccharide alginate of Pseudomonas aeruginosa, BMC Microbiol. 13 (2013), https://doi.org/10.1186/1471-2180-13-159.

[16] S. Qin, W. Xiao, C. Zhou, Q. Pu, X. Deng, L. Lan, H. Liang, X. Song, M. Wu, Pseudomonas aeruginosa: pathogenesis, virulence factors, antibiotic resistance, interaction with host, technology advances and emerging therapeutics, Signal. Transduct. Target. Ther. 7 (2022) 1–27, https://doi.org/10.1038/s41392-022-01056-1.

[17] S. Uysal, G. Zengin, M. Locatelli, M.B. Bahadori, A. Mocan, G. Bellagamba, E. De Luca, A. Mollica, A. Aktumsek, Cytotoxic and enzyme inhibitory potential of two potentilla species (P. speciosa L. and P. reptans Willd.) and their chemical composition, Front. Pharmacol. 8 (2017) 1–11, https://doi.org/10.3389/fphar.2017.00290.

[18] D.D. Milinčić, B.B. Vidović, U.M. Gašić, M. Milenković, A.Ž. Kostić, S.P. Stanojević, T. Ilić, M.B. Pešić, A systematic UHPLC Q-ToF MS approach for the characterization of bioactive compounds from freeze-dried red goji berries (L. barbarum L.) grown in Serbia: phenolic compounds and phenylamides, Food Chem. 456 (2024) 140044, https://doi.org/10.1016/j.foodchem.2024.140044.

[19] T. Tsukatani, H. Suenaga, M. Shiga, K. Noguchi, M. Ishiyama, T. Ezoe, K. Matsumoto, Comparison of the WST-8 colorimetric method and the CLSI broth microdilution method for susceptibility testing against drug-resistant bacteria, J. Microbiol. Methods 90 (2012) 160–166, https://doi.org/10.1016/j.mimet.2012.05.001.

[20] T. Li, L. Zhang, M. Cheng, E. Hu, Q. Yan, Y. Wu, W. Luo, H. Su, Z. Yu, X. Guo, Q. Chen, F. Zheng, H. Li, W. Zhang, T. Tang, J. Luo, Y. Wang, Metabolomics integrated with network pharmacology of blood-entry constituents reveals the bioactive component of Xuefu Zhuyu decoction and its angiogenic effects in treating traumatic brain injury, Chin. Med. 19 (2024) 1–16, https://doi.org/10.1186/s13020-024-01001-0 (United Kingdom).

[21] F. Hashemi-Shahraki, B. Shareghi, S. Farhadian, E. Yadollahi, A comprehensive insight into the effects of caffeic acid (CA) on pepsin: multi-spectroscopy and MD simulations methods, Spectrochim. Acta A Mol. Biomol. Spectrosc. 289 (2023) 122240, https://doi.org/10.1016/j.saa.2022.122240.

[22] W. Liu, Y. Han, J. An, S. Yu, M. Zhang, L. Li, X. Liu, H. Li, Alternation in sequence features and their influence on the anti-inflammatory activity of soy peptides during digestion and absorption in different enzymatic hydrolysis conditions, Food Chem. 471 (2025), https://doi.org/10.1016/j.foodchem.2025.142824.

[23] Y. Wang, S. Guo, W. Sun, H. Tu, Y. Tang, Y. Xu, R. Guo, Z. Zhao, Z. Yang, J. Wu, Synthesis of 4H-pyrazolo[3,4-d]pyrimidin-4-one hydrazine derivatives as a potential inhibitor for the self-assembly of TMV particles, J. Agric. Food Chem. 72 (2024) 2879–2887, https://doi.org/10.1021/acs.jafc.3c05334.

[24] Y. Hu, Q. Zhang, X. Bai, L. Men, J. Ma, D. Li, M. Xu, Q. Wei, R. Chen, D. Wang, X. Yin, T. Hu, T. Xie, Screening and modification of (+)-germacrene A synthase for the production of the anti-tumor drug (−)-β-elemene in engineered Saccharomyces cerevisiae, Int. J. Biol. Macromol. 279 (2024) 135455, https://doi.org/10.1016/j.ijbiomac.2024.135455.

[25] E. Krieger, G. Vriend, YASARA view - molecular graphics for all devices - from smartphones to workstations, Bioinformatics 30 (2014) 2981–2982, https://doi.org/10.1093/bioinformatics/btu426.

[26] M. Kabier, N. Gambacorta, D. Trisciuzzi, S. Kumar, O. Nicolotti, B. Mathew, MzDOCK: a free ready-to-use GUI-based pipeline for molecular docking simulations, J. Comput. Chem. 45 (2024) 1980–1986, https://doi.org/10.1002/JCC.27390.

[27] S. McNicholas, E. Potterton, K.S. Wilson, M.E.M. Noble, Presenting your structures: the CCP4mg molecular-graphics software, Acta Crystallogr. D Biol. Crystallogr. 67 (2011) 386–394, https://doi.org/10.1107/S0907444911007281.

[28] E.F. Pettersen, T.D. Goddard, C.C. Huang, E.C. Meng, G.S. Couch, T.I. Croll, J. H. Morris, T.E. Ferrin, U.C.S.F. ChimeraX, Structure visualization for researchers, educators, and developers, Protein Sci. 30 (2021) 70–82, https://doi.org/10.1002/pro.3943.

[29] I.M. Yusoff, Z. Mat Taher, Z. Rahmat, L.S. Chua, A review of ultrasound-assisted extraction for plant bioactive compounds: phenolics, flavonoids, thymols, saponins and proteins, Food Res. Int. 157 (2022) 111268, https://doi.org/10.1016/j.foodres.2022.111268.

[30] H.M. Rind, Proximate, phytochemical and vitamin compositions of cucumis metuliferus Proximate, phytochemical and vitamin compositions of cucumis metuliferus (Horned Melon) rind, (2020). 10.9734/jocamr/2020/v9i330144.

[31] A. del Olmo, J. Calzada, M. Nuñez, Benzoic acid and its derivatives as naturally occurring compounds in foods and as additives: uses, exposure, and controversy, Crit. Rev. Food Sci. Nutr. 57 (2017) 3084–3103, https://doi.org/10.1080/10408398.2015.1087964.

[32] A. Malik, A. Khatkar, S. Kakkar, A review on pharmacological activities of vanillic acid and its derivatives, Indo Glob. J. Pharm. Sci. 13 (2023) 01–12, https://doi.org/10.35652/igjps.2023.13001.

[33] S.K. Bhattamisra, K.H. Yap, V. Rao, H. Choudhury, Multiple biological effects of an iridoid glucoside, catalpol and its underlying molecular mechanisms, Biomolecules 10 (2020) 1–34, https://doi.org/10.3390/biom10010032.

[34] L. Zhang, H. Shi, X. Tan, Z. Jiang, P. Wang, J. Qin, Ten-gram-scale mechanochemical synthesis of ternary lanthanum coordination polymers for antibacterial and antitumor activities, Front. Chem. 10 (2022) 1–11, https://doi.org/10.3389/fchem.2022.898324.

[35] J. South, o f phytom In vitro antimicro obial activ vity of Cu ucumis metuliferus me s E . Mey . Ex . Naud din Fruit Extrac cts agains st Salmon nella galli linarum of Plant, 6 (2014) 268–274.

[36] ElsaF. Vieira, Clara Grosso, Francisca Rodrigues, ManuelaM. Moreira, VirgíniaCruz Fernandes, and Cristina Delerue-Matos (2021). Bioactive compounds of horned melon (*Cucumis metuliferus* E. Meyer ex Naudin). 10.1007/978-3-030-57415-4_21.

[37] O. Šovljanski, V. Šeregelj, L. Pezo, V.T. Šaponjac, J. Vulić, T. Cvanić, S. Markov, G. Ćetković, J. Čanadanović-Brunet, Horned melon pulp, peel, and seed: new insight into phytochemical and biological properties, Antioxidants 11 (2022), https://doi.org/10.3390/antiox11050825.

[38] H. Kaur, M. Kalia, V. Singh, V. Modgil, B. Mohan, N. Taneja, In silico identification and characterization of promising drug targets in highly virulent uropathogenic *Escherichia coli* strain CFT073 by protein-protein interaction network analysis, Inform. Med. Unlocked 25 (2021) 100704, https://doi.org/10.1016/j.imu.2021.100704.

[39] N. Høiby, Recent advances in the treatment of Pseudomonas aeruginosa infections in cystic fibrosis, BMC Med. 9 (2011), https://doi.org/10.1186/1741-7015-9-32.

[40] E. Hu, Z. Li, T. Li, X. Yang, R. Ding, H. Jiang, H. Su, M. Cheng, Z. Yu, H. Li, T. Tang, Y. Wang, A novel microbial and hepatic biotransformation-integrated network pharmacology strategy explores the therapeutic mechanisms of bioactive herbal products in neurological diseases: the effects of Astragaloside IV on intracerebral hemorrhage as an example, Chin. Med. 18 (2023) 1–18, https://doi.org/10.1186/s13020-023-00745-5 (United Kingdom).

[41] C. Liao, X. Huang, Q. Wang, D. Yao, W. Lu, Virulence factors of Pseudomonas Aeruginosa and antivirulence strategies to combat its drug resistance, Front. Cell Infect. Microbiol. 12 (2022) 1–17, https://doi.org/10.3389/fcimb.2022.926758.

[42] S. Sadeghi-kaji, B. Shareghi, A.A. Saboury, S. Farhadian, Investigating the interaction of porcine pancreatic elastase and propanol: a spectroscopy and molecular simulation study, Int. J. Biol. Macromol. 146 (2020) 687–691, https://doi.org/10.1016/j.ijbiomac.2019.12.119.

[43] S. Sadeghi-Kaji, B. Shareghi, A.A. Saboury, S. Farhadian, Spermine as a porcine pancreatic elastase activator: spectroscopic and molecular simulation studies,

J. Biomol. Struct. Dyn. 38 (2020) 78–88, https://doi.org/10.1080/07391102.2019.1568306.
[44] S. Sadeghi-kaji, B. Shareghi, A.A. Saboury, S. Farhadian, Investigation on the structure and function of porcine pancreatic elastase (PPE) under the influence of putrescine: a spectroscopy and molecular simulation study, J. Mol. Liq. 289 (2019) 111115, https://doi.org/10.1016/j.molliq.2019.111115.
[45] M. Abdollahi-Najafabadi, S. Farhadian, B. Shareghi, S. Asgharzadeh, The investigation of the interaction determination between carbendazim and elastase, using both in vitro and in silico methods, Spectrochim. Acta A Mol. Biomol. Spectrosc. 319 (2024) 124586, https://doi.org/10.1016/j.saa.2024.124586.
[46] K. Shang, C. Ge, Y. Zhang, J. Xiao, S. Liu, Y. Jiang, An evaluation of sex-specific pharmacokinetics and bioavailability of kokusaginine: an In vitro and In vivo investigation, Pharmaceuticals 17 (2024) 1–19, https://doi.org/10.3390/ph17081053.